



## Characterization of CdZnTe after argon ion beam bombardment

H. Bensalah<sup>a,\*</sup>, V. Hortelano<sup>b</sup>, J.L. Plaza<sup>a</sup>, O. Martínez<sup>b</sup>, J. Crocco<sup>a</sup>, Q. Zheng<sup>a</sup>, V. Carcelen<sup>a</sup>, E. Dieguez<sup>a</sup>

<sup>a</sup>Departamento de Física de Materiales, Laboratorio de Crecimiento de Cristales, Facultad de Ciencias, Universidad Autónoma de Madrid, Cantoblanco, 28049 Madrid, Spain

<sup>b</sup>GdS-Optronlab Group, Departamento Física Materia Condensada, Universidad de Valladolid, Edificio I+D, Paseo de Belén 1, 47011 Valladolid, Spain

### ARTICLE INFO

#### Article history:

Received 6 March 2012

Received in revised form 19 July 2012

Accepted 21 July 2012

Available online 28 July 2012

#### Keywords:

Argon ion sputtering

CdZnTe

Te inclusions

### ABSTRACT

The objective of this work is to analyze the effects of argon ion irradiation process on the structure and distribution of Te inclusions in  $\text{Cd}_{1-x}\text{Zn}_x\text{Te}$  crystals. The samples were treated with different ion fluences ranging from 2 to  $8 \times 10^{17} \text{ cm}^{-2}$ . The state of the samples before and after irradiation were studied by Scanning Electron Microscopy (SEM), Atomic Force Microscopy (AFM), Cathodoluminescence, Photoluminescence, and micro-Raman spectroscopy. The effect of the irradiation on the surface of the samples was clearly observed by SEM or AFM. Even for small fluences a removal of polishing scratches on the sample surfaces was observed. Likely correlated to this effect, an important enhancement in the luminescence intensity of the irradiated samples was observed. An aggregation effect of the Te inclusions seems to occur due to the Ar bombardment, which are also eliminated from the surfaces for the highest ion fluences used.

© 2012 Elsevier B.V. All rights reserved.

### 1. Introduction

CdZnTe (CZT) crystals can be used in a variety of detector-type applications. This is due to several interesting material properties including large absorption coefficient, high resistivity, high average atomic number, and large band gap [1]. As a consequence of these properties, CZT is a very promising material for its use as room temperature gamma detector. Historically, the performance of CZT has typically been adversely affected by point defects, structural and compositional heterogeneities within the crystals, such as twinning, pipes, grain boundaries and Te inclusions, etc. Te inclusions and precipitates are created during the growth and the cooling down phases [2]. They are the result of the retrograde solid solubility of Te and, in general, they are created when the growth system offers a poor stoichiometric control [3]. The concentration and distribution of Te inclusions within a device are one of the major contributions to the degradation of CZT detectors. Te precipitates on the surface can also increase the leakage current [4,5], thereby deteriorating the device performance. Te inclusions and precipitates also act as traps for the charge carriers. This trapping affects the charge collection efficiency as well as the energy resolution of the detector. For this reason it is necessary to study these defects and adopt appropriate techniques to minimize their influence. The main goal of our work is to ascertain the effect of one of such techniques, namely, Ion beam sputtering (IBS) on the formation, evolution and clustering of Te inclusions in CZT. It is well known that Te inclusions are spread all over the bulk of CZT

crystals [6,7]. However, in spite of the fact that IBS is a surface technique, the enhancement of the surface properties by this method is expected to improve the contact formation of the devices.

Ion beam sputtering (IBS) has come to play an important role in science and technology. The sputtering phenomenon is caused by the interaction of incident particles with the target surface atoms. IBS is employed in many applications, such as ion doping, surface cleaning and etching, thin film deposition, ion milling [8,9], etc. Some important results have been reported by different authors about the effect of argon irradiation on the surface of different semiconductors like GaSb, CdTe and CdZnTe. For instance, Panin et al. [8] used argon ion sputtering to induce conductivity changes on GaSb crystals. Panin et al. [9] also reported the formation of an n-type surface layer on p-type CdTe crystals, which is caused by the suppression of vacancies acting as the main acceptors in these crystals. J. Olvera et al. demonstrated that the luminescent properties of CdTe substrates can be very much increased after irradiation with low energy argon ions; this enhancement is due to the removal of surface damage produced after sample cutting and polishing processes [10,11]. Voss et al. reported that the Ar ion bombardment of  $\text{Cd}_{0.46}\text{Zn}_{0.04}\text{Te}_{0.50}$  results in a modified surface atomic ratio, with Cd being preferentially removed compared to Te; in addition, the native oxide is removed and the leakage current decreases approximately 2.5 orders of magnitude compared to non-irradiated samples [12].

In this work, we describe the effects of argon ion beam bombardment at different fluences on the surface composition, luminescence properties and Te inclusions of  $\text{Cd}_{0.9}\text{Zn}_{0.1}\text{Te}$  crystals. The analysis is carried out by combining different techniques:

\* Corresponding author.

E-mail address: [hakima.bensalah@uam.es](mailto:hakima.bensalah@uam.es) (H. Bensalah).

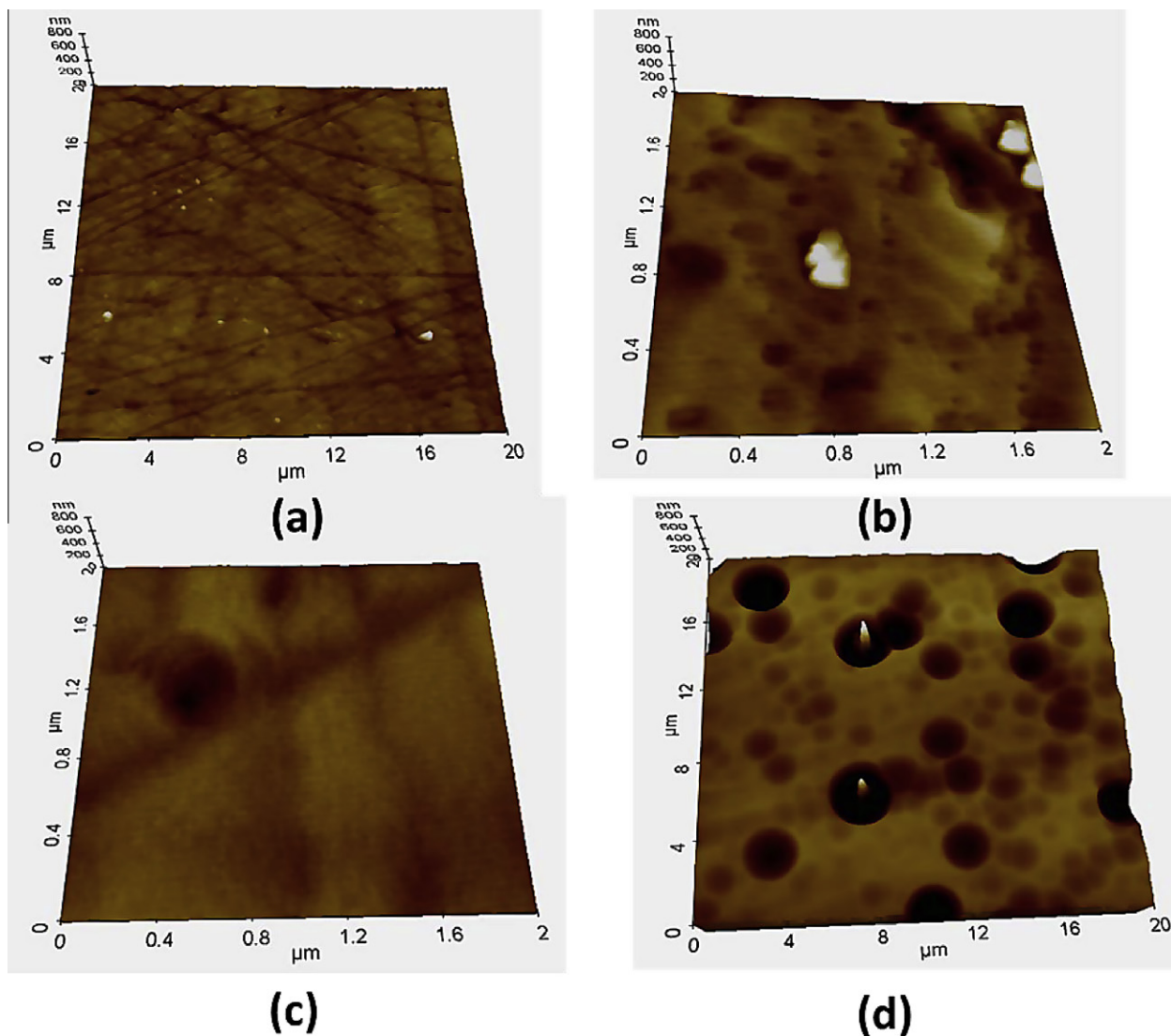


Fig. 1. AFM images of CZT samples: no irradiated (a) and irradiated with fluences of  $2 \times 10^{17} \text{ cm}^{-2}$  (b),  $4 \times 10^{17} \text{ cm}^{-2}$  (c) and  $8 \times 10^{17} \text{ cm}^{-2}$  (d).

Scanning Electron Microscopy (SEM), Atomic Force Microscopy (AFM), Cathodoluminescence, Photoluminescence, and micro-Raman spectroscopy.

## 2. Experimental details

### 2.1. Sample preparation

$\text{Cd}_{0.9}\text{Zn}_{0.1}\text{Te}$  crystals were grown by the vertical Bridgman method.  $8 \times 5 \times 2 \text{ mm}^3$  samples were cut from the grown ingot and then lapped and polished by using  $3 \mu\text{m}$   $\text{Al}_2\text{O}_3$  powder [1]. Several samples cut from the same position along the ingot were irradiated. A Specs PQ10 broad beam ion gun was used for the ion irradiation. A filament current of 10 mA with an energy of 5 keV was selected. Three sputtering times were studied: 1, 3 and 8 h, which resulted in fluences of  $2$ ,  $4$ , and  $8 \times 10^{17} \text{ cm}^{-2}$ , respectively.

### 2.2. Characterization

The samples were characterized before and after irradiation using a Scanning Electron Microscope (Hitachi S-3000 N) for surface quality. An Atomic Force Microscope (PSI100 Park Systems) was used for analyzing surface roughness. Micro-photoluminescence ( $\mu\text{PL}$ ) and micro-Raman ( $\mu\text{R}$ ) spectra were obtained with a HRLabRam spectrometer attached to a metallographic microscope. The excitation was done with an He–Ne laser line at 633 nm, through a  $100\times$  microscope objective, which also collected the scattered light. CL measurements (panchromatic

images as well as CL spectra) were carried out at liquid nitrogen temperature (80 K) with a XiCLOne system (Gatan UK) attached to a LEO 1530-Carl Zeiss FESEM microscope. The luminescence signal was detected with a Peltier cooled CCD.

## 3. Results and discussion

Fig. 1 shows the AFM images of the irradiated surfaces with fluences of  $2$ ,  $4$  and  $8 \times 10^{17} \text{ cm}^{-2}$ . From these images we can infer different surface structural development regimes. The scratches observed in the polished crystals are removed for all the fluences used in this study, thus leading to a cleaner surface. For instance, the surface roughness before irradiation is  $\sim 10 \text{ nm}$  (Fig. 1a), while the surface roughness of the clean areas after irradiation with the maximum fluence is  $\sim 5.5 \text{ nm}$  (Fig. 1d). An additional effect has been observed as the irradiation fluence increases; after irradiation with the lower fluence ( $2 \times 10^{17} \text{ cm}^{-2}$ ) we observe the generation of pitting on the surface while for medium ( $4 \times 10^{17} \text{ cm}^{-2}$ ) fluence surface waviness is observed. For the highest fluence, deeper holes start to form on the surface accompanied by a rough surface with the formation of two kinds of pits: (i) void craters and (ii) craters with a particle in the middle. SEM images of the surface of the sample irradiated at the highest fluence are presented in Fig. 2. The above mentioned pits created by the ion beam can be clearly

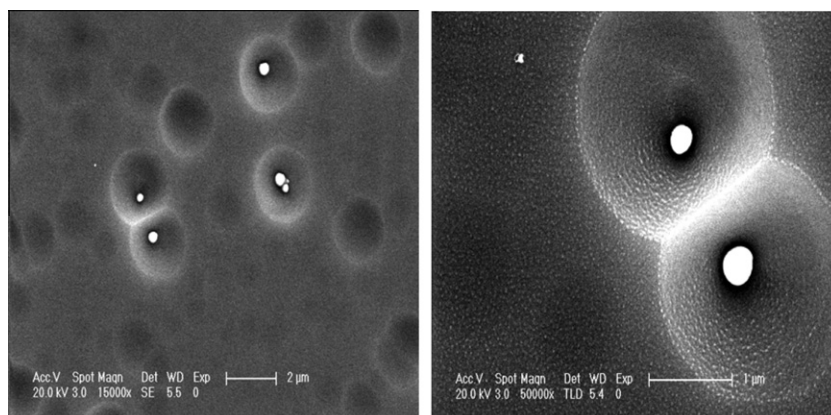


Fig. 2. SEM images of the sample irradiated with a fluence of  $8 \times 10^{17} \text{ cm}^{-2}$ .

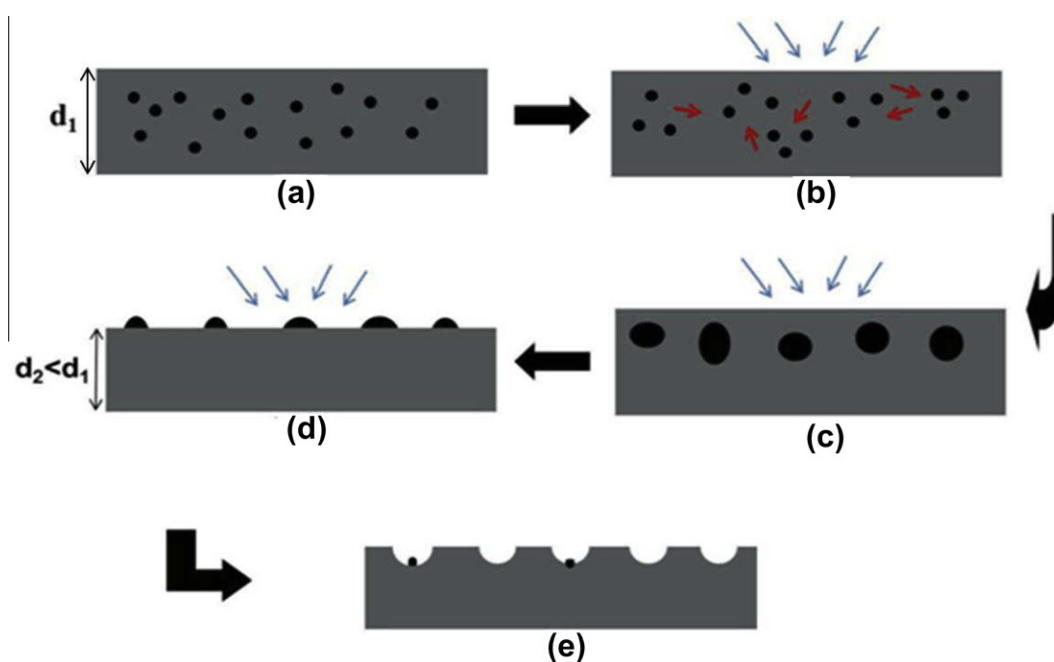


Fig. 3. Schematic representation of the elimination of Te inclusions during the bombardment with argon ions ( $d_1$  is referred to the surface layer of the sample, as the IBS is a surface process).

observed here. The typical size of the craters and the nanoparticles is about 2 and 0.5  $\mu\text{m}$ , respectively.

The formation of these two different kinds of structures is illustrated in Fig. 3 and could be explained as follows: (a) we assume that our starting CZT crystals are rich in excess Te, so a high amount of Te interstitials ( $\text{Te}_i$ ) and/or Cd vacancies ( $\text{V}_{\text{Cd}}$ ) are present in the material, as well as a random distribution of Te inclusions and precipitates in the sample volume [13]; (b) the ion bombardment process implies to supply energy to the crystal lattice, which can locally increase the segregation coefficient of Te in the volume affected by the irradiation process, thus allowing for an extra formation of Te aggregates; (c) in consequence larger Te clusters could be created; (d) as the surface is eroded some of the Te cluster, those close to the surface, are unburied and exposed to the ion beam; (e) as these clusters are different material (pure Te) than the surroundings (CZT), the sputtering yields are also different for both; it happens that the sputtering yield for Te is higher than CZT [14]. As the Te are more “resistive” to the ion erosion than CZT, the Te clusters act like small “masks” and the surroundings are eroded faster than the clusters leading to the crater formation. Those craters with a Te cluster inside are those in which the ion

beam did not have time for the complete erosion of the cluster; in those cases, the central part presents a peak, as is observed in the AFM image of Fig. 1d.

A detailed study of the optical properties of the irradiated and no irradiated samples was performed by means of luminescence and Raman techniques. Fig. 4 shows the RT-PL spectra of the CdZnTe samples obtained at both irradiated and no irradiated areas. The PL spectra are composed of a single broad peak at energy close to the band gap. The important difference concerns the peak intensity, which greatly increases after irradiation. This increase should be related to the improved quality of the CdZnTe surfaces after irradiation, due to the removal of the surface defects created during the cutting, lapping, and polishing processes. The PL peak position also blueshifts after the irradiation process, this effect being more marked for increasing fluences. This should be likely related to a depletion of Cd atoms in the surface after the irradiation process, leading to a CdZnTe alloy with an increased Zn content and a decreased Cd content.

The luminescence properties of the sample have been also studied by means of low temperature (80 K) Cathodoluminescence (CL) spectroscopy. Fig. 5 shows the CL spectra of both irradiated and no

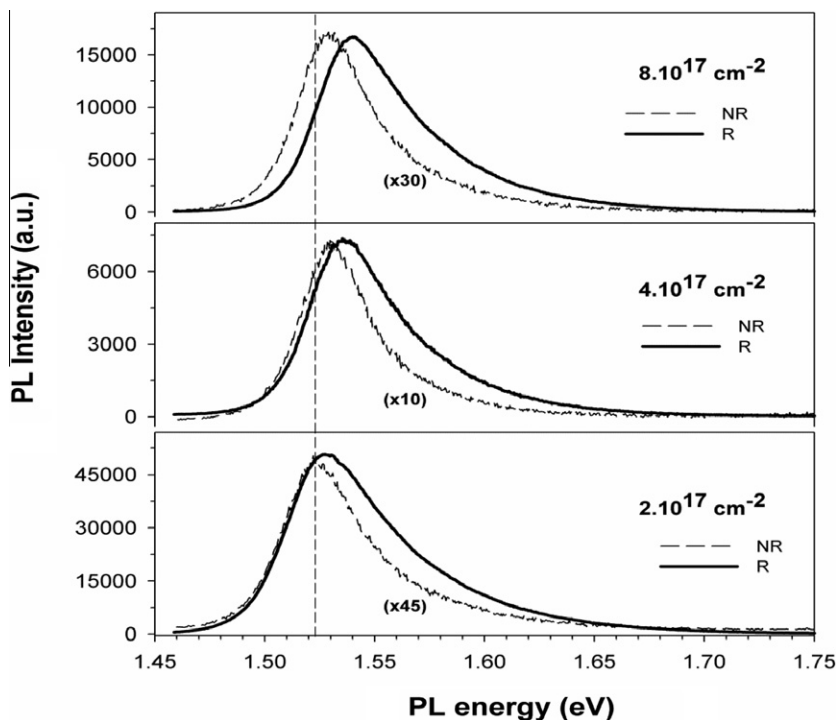


Fig. 4. PL spectra of the studied CdZnTe samples at both irradiated (R) and no irradiated (NR) areas for different fluences:  $2 \times 10^{17} \text{ cm}^{-2}$ ,  $4 \times 10^{17} \text{ cm}^{-2}$ , and  $8 \times 10^{17} \text{ cm}^{-2}$ .

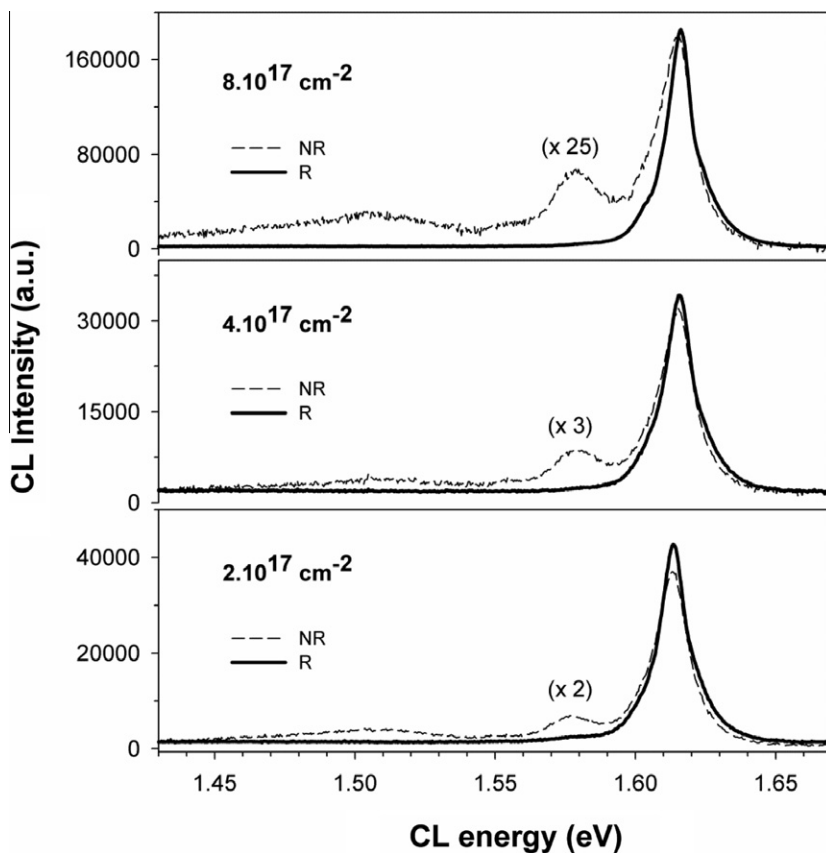


Fig. 5. CL spectra of the CdZnTe samples at both irradiated (R) and no irradiated (NR) areas for different fluences: (a)  $2 \times 10^{17} \text{ cm}^{-2}$ , (b)  $4 \times 10^{17} \text{ cm}^{-2}$ , (c)  $8 \times 10^{17} \text{ cm}^{-2}$ .

irradiated areas. The CL spectrum of the CdZnTe samples before irradiation shows (i) a prominent acceptor bound exciton transi-

tion ( $A^\circ, X$ ) at 1.61 eV, (ii) an emission at 1.57 eV, with the characteristics of free to bound acceptor transition ( $eA^\circ$ ), and (iii) a weak

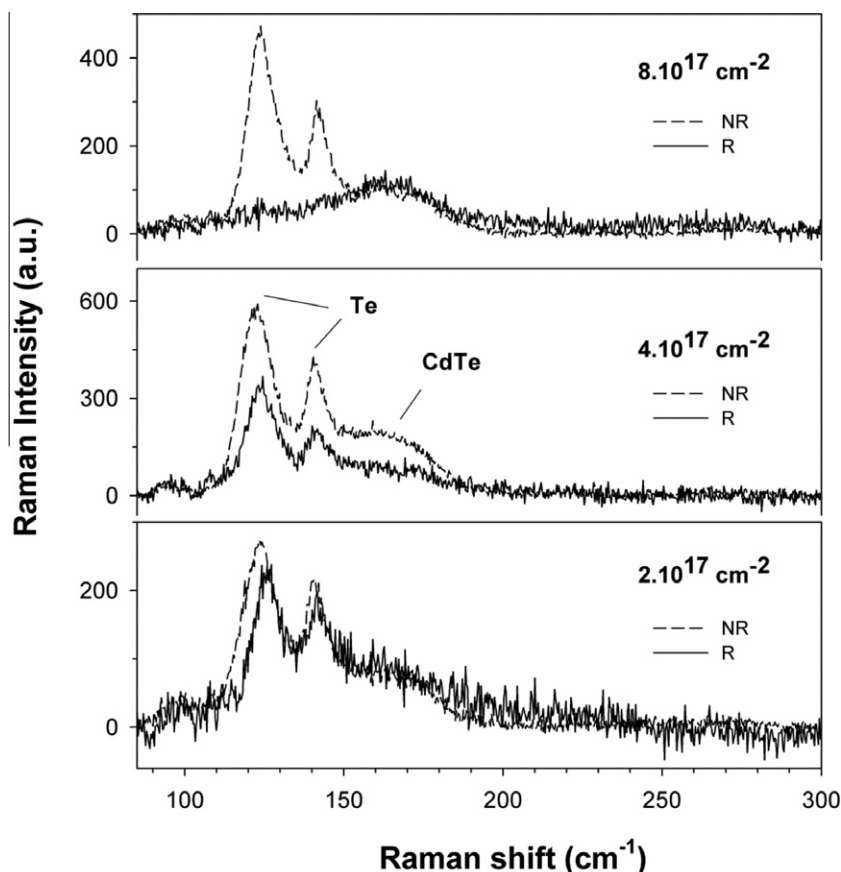


Fig. 6. Raman spectra of irradiated (R) and no irradiated (NR) areas for the different fluences investigated.

broad emission at 1.49 eV, related to surface defects [15]. After irradiation we observe both an increase of the intensity of the excitonic emission as well as a decrease of its full width at half maximum, these effects being more marked for the highest fluence used. Also, we observe that the broad band at 1.49 eV was removed after irradiation for all the analyzed fluences. These observations support again the removal of surface defects due to the Ar irradiation process. On the other hand, the CL peak at 1.57 eV is observed to be slightly reduced after irradiation with a fluence of  $2 \times 10^{17} \text{ cm}^{-2}$ , while it completely disappears when using higher fluences.

Finally, typical Raman spectra of the irradiated and no irradiated CdZnTe areas of the studied samples are presented in Fig. 6. The Raman peaks at 123 and 141  $\text{cm}^{-1}$ , observed with great intensities for the no irradiated areas, are attributed to the presence of Te inclusions [16]. It is observed that the intensities of both peaks decrease after irradiation, for all the fluences used, although the change is better observed as the fluence increases. In fact, the irradiation with the smallest fluence produces a very small reduction of the intensities of these two peaks, while for the highest fluence used the two Raman peaks disappear completely. This indicates that the irradiation process leads to an elimination of Te precipitates from the surfaces of the CdZnTe samples, as has been previously mentioned in our model depicted in Fig. 3.

#### 4. Conclusions

The surface of CZT crystals before and after argon ion bombardment was investigated by topographic and optical techniques. The results of the irradiated samples show an improvement of the quality of the crystal by means of a reduction of surface defects,

which is also deduced from the increase of the band-to-band luminescence intensity and the diminution of the luminescence band at 1.49 eV, usually related to extended surface defects. Moreover, the ion bombardment seems to produce accumulation of Te inclusions, some of them visible on the surface of the samples. The use of elevated fluences leads to a higher diminution of the Te aggregates, as deduced from the Raman spectra of the surfaces. Therefore, this work provides new relevant information on changes in the physical properties of CZT surfaces and their relationship with Te inclusion dynamics under low energy  $\text{Ar}^+$  ion irradiation.

#### Acknowledgments

This work was partially supported by the following Projects: MAT 2009-08582, Spanish “Ministerio de Ciencia e Innovación”; FP7-SEC-2007-01, “Cooperation across Europe for Cd(Zn)Te based Security Instrument”, COCAE.

#### References

- [1] H. Bensalah, J.L. Plaza, J. Crocco, Q. Zheng, V. Carcelen, A. Bensouici, E. Diéguez, *Appl. Surf. Sci.* 257 (2011) 4633.
- [2] P. Rudolph, *Cryst. Res. Technol.* 38 (2003) 542.
- [3] Robert Triboulet, Paul Siffert, CdTe and Related Compounds; Physics, Defects, Hetero- and Nano-structures, Crystal Growth, Surfaces and Applications (European Materials Research Society Series), Institute of Leadership & Mana, The Netherlands, 2010.
- [4] T. Wang, W. Jie, D. Zeng, *Mater. Sci. Eng. A* 472 (2008) 227.
- [5] H.Y. Pei, J.X. Fang, *Phys. Status Solidi A* 188 (2001) 1161.
- [6] A.E. Bolotnikov, G.S. Camarda, G.A. Carini, Y. Cui, K.T. Kohman, L. Li, M.B. Salomon, R.B. James, *IEEE Trans. Nucl. Sci.* 54 (1997) 821.
- [7] S. Derek, J. Bale, *Appl. Phys.* 108 (2010) 024504.
- [8] G.N. Panin, P.S. Dutta, J. Piqueras, E. Dieguez, *Appl. Phys. Lett.* 67 (1995) 3584.
- [9] G. Panin, P. Fernandez, J. Piqueras, *Semicond. Sci. Technol.* 11 (1996) 1354.

- [10] J. Olvera, O. Martínez, M. Avella, J.L. Plaza, S. de Dios, E. Diéguez, J. Appl. Phys. 108 (2010) 123513.
- [11] J. Olvera, O. Martínez, J.L. Plaza, E. Dieguez, J. Lumin. 129 (2009) 941.
- [12] L.F. Voss, P.R. Beck, A.M. Conway, R.T. Graff, R.J. Nikolic, A.J. Nelson, S.A. Payne, J. Appl. Phys. 108 (2010) 014510.
- [13] P. Rudolph, M. Neubert, M. Miihlberg, J. Cryst. Growth 128 (1993) 582.
- [14] <<http://www.srim.org/>>
- [15] J.K. Radhakrishnan, G. Salviati, J. Lumin. 113 (2005) 235.
- [16] N.V. Sonchinskii, M.D. Serrano, E. Diéguez, F. Agulló-Rueda, U. Pal, J. Piqueras, P. Fernández, J. App. Phys. 77 (1995) 2806.